ELSEVIER

Thermochimica Acta 285 (1996) 99–107

thermochimica acta

Thermal studies of 2-aminoethanol complexes of nickel (II) in the solid state

Debasis Das, Ashutosh Ghosh [1], Subratanath Koner, Nirmalendu Ray Chaudhuri *

Department of Inorganic Chemistry, Indian Association for the Cultivation of Science, Calcutta 700 032, India

Received 22 August 1995; accepted 29 January 1996

Abstract

$[NiL_3]X_2$ (where L = 2-aminoethanol and X is Cl^-, Br^-, I^-, NO_3^-, $0.5SO_4^{2-}$ or $0.5SeO_4^{2-}$) and $[NiL_2X_2]$ (X is Cl^-, Br^-, or SCN^-) have been synthesised from solution and their thermal study has been carried out in the solid phase. $[NiL_3]I_2$ and $[NiL_3]SeO_4$ undergo reversible endothermic phase transitions upon heating (63–93°C and 94–113°C, respectively, for heating and 94–65°C and 110–190°C, respectively, for cooling), whereas $[NiL_3](NO_3)_2$ exhibits two successive reversible endothermic phase transitions (10–38°C and 50–62°C for heating and 56–48°C and 19 – (–8)°C for cooling). On the other hand, $[NiL_3]SO_4$ undergoes irreversible endothermic phase transition (99–112°C) in the solid state. All these transformations are assumed to be associated with the conformational changes of 2-aminoethanol chelate rings. $[NiL_2(NCS)_2]$ melts at ~ 168°C and remains supercooled for a few days at ambient temperature. The initial temperatures of decomposition (T_i) of these complexes have been compared with those of the corresponding ethane-1, 2-diamine complexes of nickel (II).

Keywords: DTA; Nickel compounds; Phase transition; Stability; TG

1. Introduction

Synthesis, characterisation and solid state thermal investigation of nickel(II) complexes with five-membered diamine (*N*,*N*-donor) chelate ligands are well documented [1–5]. The study reveals that some of the complexes show novel phase transition

* Corresponding author.

[1] Present Address: Department of Chemistry, Jhargram Raj College, Jhargram 721 507, West Bengal, India.

PII: S0040-6031(96)02898-5

phenomena upon heating in the solid phase. The transitions are described as being due to one of the following causes:

(1) conformational changes of the five-membered diamine chelate rings [6, 7];

(2) *cis* ⇄ *trans* isomerism [3, 8]; or

(3) octahedral ⇄ square–planar structural changes [9–11]. Moreover, some of the complexes upon heating undergo decomposition showing plateaus in their corresponding TG curves yielding novel complexes as intermediates, which may not be synthesised from solution. On the other hand, the study with the five-membered chelates formed by aminoalcohols (*N*,*O*-donors) has not yet been undertaken. This type of chelating ligand appears to be interesting owing to its hetero donor sites. 2-Aminoethanol being the simplest member of the aminoalcohol series is taken into consideration and this paper reports synthesis of 2-aminoethanol complexes of nickel (II) X_2 ($X = Cl^-, Br^-, I^-, SCN^-, NO_3^-, 0.5SO_4^{2-}$ and $0.5SeO_4^{2-}$), their characterisation and thermal investigation in the solid phase.

2. Experimental

High purity (99 + %) 2-aminoethanol (L) was purchased from Aldrich Chemical Company Inc. and used as received. All other chemicals were AR grade. Thermal analysis (TG–DTA) was carried out using Shimadzu DT-30 thermal analyser in a dynamic atmosphere of dinitrogen (flow rate: 30 $cm^3\ min^{-1}$). The sample (particle size within 150–200 mesh) was heated in a platinum crucible at a rate of 10°C min^{-1} with inert alumina as reference. The enthalpy changes of phase transitions were calculated by means of a Perkin–Elmer DSC-7 differential scanning calorimeter using indium metal as calibrant (rate of heating and/or cooling 10°C min^{-1}). Elemental analyses, IR spectra (4000–250 cm^{-1}), electronic spectra (mull) (900–190 nm) and magnetic susceptibility were measured with a Perkin–Elmer 240C elemental analyser, a Perkin–Elmer IR 783, a Shimadzu UV 2100, and EG and G PAR 155 vibrating sample magnetometer, respectively. X-ray powder diffraction patterns were taken using CuK_α radiation with a Philips X-ray generator (PW 1130) and X-ray diffractometer (PW 1130).

Commerical anhydrous nickel(II) iodide was found to be practically insoluble in ethanol. Accordingly, an ethanolic solution of nickel(II) iodide was prepared by mixing nickel(II) nitrate hexahydrate and sodium iodide in ethanol in a 1:2 molar ratio and removal of the sodium nitrate by filtration as described by Goodgame and Venanzi [12].

2.1. Preparation of the complexes

$[NiL_3]Cl_2$ (**1**), $[NiL_3]Br_2$ (**3**), $[NiL_3]I_2$ (**5**), were prepared by slow addition of an ethanolic solution (5 cm^3) of 2-aminoethanol (3mmol) to anhydrous nickel(II) salts (1 mmol) dissolved in ethanol (10 cm^3). The resulting mixture was evaporated to dryness in vaccum desiccator. The dried mass treated with ether–isopropanol (1:1) mixture, filtered and dried in a vacuum desiccator. Freshly prepared nickel(II) iodide was used for $[NiL_3]I_2$.

$[NiL_2Cl_2]$ (**2**), $[NiL_2Br_2]$ (**4**) and $[NiL_2(NCS)_2]$ (**9**) were synthesised similarly by mixing metal salts and ligand in 1:2 ratio.

$[NiL_3](NO_3)_2$ (**6**), was obtained by dropwise addition of ligand (3 mmol) in butanol ($5cm^3$) to nickel(II) nitrate (1 mmol) in butanol (10 cm^3) at $\sim 80°C$. Separation of the desired species took place immediately and the complex was filtered and washed with butanol and dried in a $CaCl_2$ desiccator.

$[NiL_3]SO_4$ (**7**), and $[NiL_3]SeO_4$ (**8**), were prepared following the method reported earlier [13].

3. Results and discussion

3.1. Characterisation of the complexes

The complexes $[NiL_3]SO_4$ and $[NiL_2X_2]$ ($X = Cl^-, Br^-, I^-, SCN^-$ and $0.5SO_4^{2-}$) were prepared by Masoud [13]. We prepared $[NiL_3]X_2$ (where $X = Cl^-$, Br^-, I^-, NO_3^-, $0.5SO_4^{2-}$ and $0.5SeO_4^{2-}$) and $[NiL_2X_2]$ (where $X = Cl^-$, Br^-, and SCN^-) as is evident from the elemental analyses (Table 1). IR spectra of the free ligand and its complexes with nickel(II) were reported earlier [13, 14]. The shifting, to the lower energy region, of IR bands appearing at 1610, 1500, 1160 and 980 cm^{-1}, due to the deformation, bending and wagging vibrations of the amino group in the free ligand, is taken as evidence that the ligand acts as a five-membered bidentate chelate. Later single crystal analysis of $[NiL_2(NCS)_2]$ [15] established the chelating charactersitics of the ligand. Similar shifts in the IR bands were observed for all the complexes reported here, which indicates that the ligand is chelated. Thereby, all tris species possess the NiN_3O_3 chromophore and bis complexes show the $NiN_2O_2X_2$ chromophore with octahedral geometry around Ni(II) as is evident from their magnetic and electronic spectral (mull) data (Table 1).

Table 1
Elemental analyses, magnetic and electronic (mull) spectral data of 2-aminoethanol (L) complexes of nickel(II)

Complex	No.	Colour	Elemental analyses/%[a]			μ_{eff}/ B.M.	λ_{max}/nm
			C	H	N		
$[NiL_3]Cl_2$	(1)	Blue–violet	22.9(23.0)	6.6(6.8)	13.2(13.4)	3.1	355, 570
$[NiL_2Cl_2]$	(2)	Green	18.8(19.1)	5.5(5.6)	11.0(11.1)	3.2	365, 590
$[NiL_3]Br_2$	(3)	Blue–violet	17.9(17.9)	5.1(5.2)	10.4(10.5)	3.1	358, 575
$[NiL_2Br_2]$	(4)	Green	14.0(14.1)	4.0(4.2)	8.2(8.2)	3.2	370, 595
$[NiL_3]I_2$	(5)	Blue–violet	14.2(14.5)	4.1(4.2)	8.3(8.5)	3.2	345, 560
$[NiL_3](NO_3)_2$	(6)	Blue–violet	19.7(19.7)	5.7(5.7)	19.1(19.1)	3.1	360, 565
$[NiL_3]SO_4$	(7)	Pink	21.3(21.3)	6.0(6.2)	12.4(12.4)	3.2	370, 610
$[NiL_3]SeO_4$	(8)	Pink	18.6(18.7)	5.4(5.5)	10.8(10.9)	3.2	365, 605
$[NiL_2(NCS)_2]$	(9)	Pink	24.3(24.3)	4.6(4.7)	18.9(18.9)	3.2	355, 578

[a] Percentages in parentheses are theoretically calculated values.

3.2. Phase transition of the complexes

Upon heating the complexes $[NiL_3]I_2$ (**5**) and $[NiL_3]SeO_4$ (**8**), undergo reversible endothermic phase transitions without showing any visual colour change (Table 2 and Fig. 1). The IR spectra (Table 3) of both (**5**) and (**8**) were taken at ambient temperature, at the temperature at which the respective phase transitions seemed to be complete, and also after cooling of the heated samples. The IR spectra taken at elevated temperature for both the complexes (**5a** and **8a**) show remarkable differences from their ambient temperature IR spectra in the regions 1500–1600, 1300–1400 cm^{-1}, 1000–1200 cm^{-1} and 800–900 cm^{-1}, where shifting of ligand band due to chelation was expected. IR spectra taken after cooling of the heated samples to ambient temperature are just replicas of the IR spectra of the low-temperature phase species, which corroborates the completely reversible nature of the phase transitions. In the case of five-membered diamine chelates, the IR spectra of the high-temperature phase species were found to be different from those of the low-temperature phase species at the positions where N–H and C–H stretching

Table 2
Thermal parameters of 2-aminoethanol (L) complexes of nickel(II)

Thermally induced reactions	Temperature range/°C	Data peak temp./°C		ΔH^b/ (kJ mol^{-1})
		Endo	Exo	
$[NiL_3]Cl_2$ (**1**) → $[NiL_2Cl_2]$	150–183	177	–	–
$[NiL_2Cl_2]$ → $NiCl_2$	183–340	–	*260*	–
$[NiL_2Cl_2]$ (**2**) → $NiL_{1.5}Cl_2$	90–142	105	–	–
$NiL_{1.5}Cl_2$ → $NiLCl_2$	142–232	230	–	–
$NiLCl_2$ → $NiCl_2$	232–340	–	270	–
$[NiL_3]Br_2$ (**3**) → $NiBr_2$	170–380	215	260	–
$[NiL_2Br_2]$ (**4**) → $NiBr_2$	210–390	240	310	–
$[NiL_3]I_2$ (**5**) → $[NiL_3]I_2$ (**5a**)[a]	63–93	80	–	3.11
$[NiL_3]I_2$ (**5a**) → $[NiL_3]I_2$ (**5**)[a]	94–65	–	74	– 2.98
$[NiL_3]I_2$ (**5a**) → NiI_2	180–335	182	220	–
$[NiL_3](NO_3)_2$ (**6**) → $[NiL_3](NO_3)_2$ (**6a**)[a]	10–38	30	–	3.83
$[NiL_3](NO_3)_2$ (**6a**) → $[NiL_3](NO_3)_2$ (**6**)[a]	19–(– 8)	–	4	– 2.85
$[NiL_3](NO_3)_2$ (**6a**) → $[NiL_3](NO_3)_2$ (**6b**)[a]	50–62	58	–	0.77
$[NiL_3](NO_3)_2$ (**6b**) → $[NiL_3](NO_3)_2$ (**6a**)[a]	56–48	–	53	– 0.69
$[NiL_3](NO_3)_2$ (**6b**) → Product not identified	170(T_i)	–	–	–
$[NiL_3]SO_4$ (**7**) → $[NiL_3]SO_4$ (**7a**)[a]	99–112	108	–	1.35
$[NiL_3]SO_4$ (**7a**) → $[NiL_2SO_4]$ (**7b**)	185–232	203	–	–
$[NiL_2SO_4]$ (**7b**) → $NiSO_4$	232–345	290	242	–
$[NiL_3]SeO_4$ (**8**) → $[NiL_3]SeO_4$ (**8a**)[a]	94–113	103	–	1.05
$[NiL_3]SeO_4$ (**8a**) → $[NiL_3]SeO_4$ (**8**)[a]	110–190	–	100	– 0.97
$[NiL_3]SeO_4$ (**8a**) → $NiSeO_4$	210–248	222	230	–
$[NiL_2(NCS)_2]$ (**9**) → $[NiL_2(NCS)_2]$	155–185	168	–	–
$[NiL_2(NCS_2)]$ → $Ni(NCS)_2$	215–340	–	225	–

[a] Temperature range obtained from DSC.
[b] The standard deviations for ΔH values = $\pm$ 0.2kJ mol^{-1}.

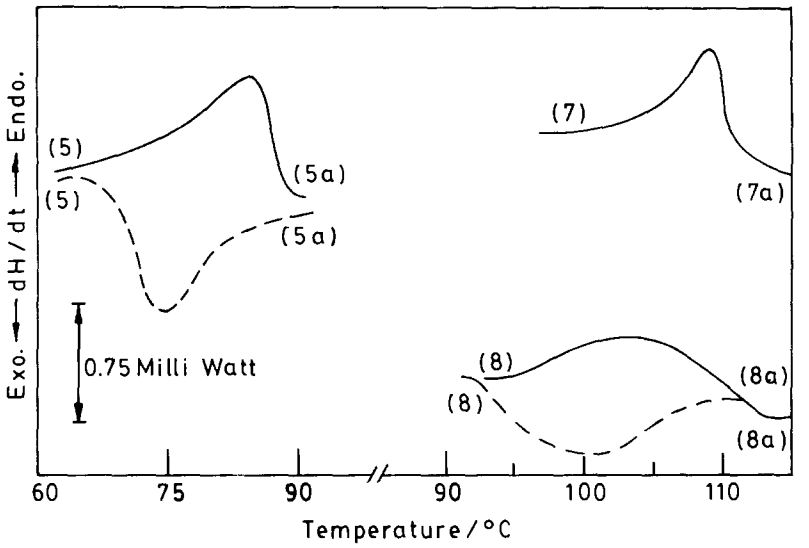

Fig. 1. DSC curves: $[NiL_3]I_2$ (**5**) (sample mass, 8.23 mg); $[NiL_3]SO_4$ (**7**) (sample mass, 10.52 mg) and $[NiL_3]SeO_4$ (**8**) (sample mass, 10.62 mg); (heating cycle, – –; cooling cycle, ----).

Table 3
IR spectral data (nujol) of 2-aminoethanol (L) complexes of nickel(II)

Complex[a]	IR bands (cm^{-1})[b]
$[NiL_3]I_2$ (**5**)	3300(sbr), 3150(sbr), 1590(s), 1460(w), 1450(w), 1410(w), 1370(w), 1310(s), 1290(w), 1230(w), 1190(w), 1110(s), 1050(s), 1015(s), 880(s), 855(w)
$[NiL_3]I_2$ (**5a**)	3260(sbr), 3140(wbr)1595(s), 1455(w), 1360(w), 1280(s), 1185(w), 1055(s), 1005(s), 865(w)
$[NiL_3](NO_3)_2$ (**6**)	3250(sbr), 2940(sbr), 1790(s), 1750(w), 1600(s), 1455(w), 1375(w), 1115(s), 1055(s), 1015(s), 875(s), 835(s)
$[NiL_3]SO_4$ (**7**)	3440(sbr), 3280(s), 3160(s), 2900(s), 2850(s), 1790(s), 1595(s), 1455(s), 1375(s), 1155(s), 1118(s), 1055(s), 1030(w), 1015(w), 985(s), 885(s), 835(s),
$[NiL_3]SO_4$ (**7a**)	3260(sbr), 3140(wbr), 2940(s), 2820(w), 1785(s), 1595(s), 1455(s), 1125(wbr), 1050(s), 1000(s), 880(s), 835(s),
$[NiL_3]SeO_4$ (**8**)	3275(sbr), 3150(wbr), 2920(wbr), 2850(s), 1605(s), 1460(s), 1380(s), 1345(w), 1325(w), 1310(w), 1270(w), 1125(s), 1055(s), 1015(s), 870(w), 845(w)
$[NiL_3]SeO_4$ (**8a**)	3220(s), 3140(sbr), 2910(wbr), 2840(s), 1595(s), 1480(w), 1375(s), 1330(sbr), 1265(w), 1125(wbr), 1055(sbr), 1020(s), 860(s)

[a] IR spectral band positions of complexes (**1**), (**2**), (**3**) and (**4**) are not shown owing to their similarity to complex (**5**).

[b] s, strong; w, weak; br, broad.

and bending vibrations were assigned and it was concluded that this type of isomerization was due to conformational changes of the diamine chelate rings [16–18]. Thus conformational isomerism is assumed to be responsible for the phase transitions in these complexes (**5** and **8**).

$[NiL_3](NO_3)_2$ (**6**) exhibits two successive reversible phase transitions upon heating (Table 2 and Fig. 2) without showing any visual colour change. The enthalpy values and the temperature ranges for the phase transitions are reproducible. The lower ΔH values and the broad nature of the exothermic peak in the cooling curve hints that the reversion takes place slowly and is not complete in the temperature range of the exothermic peak. IR spectral study was also performed in the same manner as for (**5**) and (**8**). But no remarkable change in the IR spectra were obtained for the low- and high-temperature phase species. As a result it is difficult to comment whether the conformational changes of the chelate rings take place or not.

$[NiL_3]SO_4$ (**7**) undergoes an irreversible endothermic phase transition (Table 2 and Fig. 1) upon heating, yielding (**7a**) without showing any colour change. XRD data of (**7**) and (**7a**) (Table 4) differ considerably. IR spectra of (**7**) and (**7a**) also differ in the same region as described for (**5**) and (**8**). This reveals that here also phase transition is presumed to be due to the conformational changes of the chelate rings.

$[NiL_2(NCS)_2]$ (**9**) melts at ~ 168°C without showing any mass loss in the TG curve. After cooling, to ambient temperature the sample is reheated immediately, but no melting phenomenon is observed to take place at the same temperature range. If the molten sample is kept in a $CaCl_2$ desiccator at ambinet temperature for a few days and then reheated, the melting peak is again observed in the same temperature range.

3.3. Thermal decomposition

All tris complexes of nickel(II) decompose immediately upon heating to their corresponding salt, expcept for $[NiL_3]Cl_2$ (**1**) and $[NiL_3]SO_4$ (**7**) which show plateaus

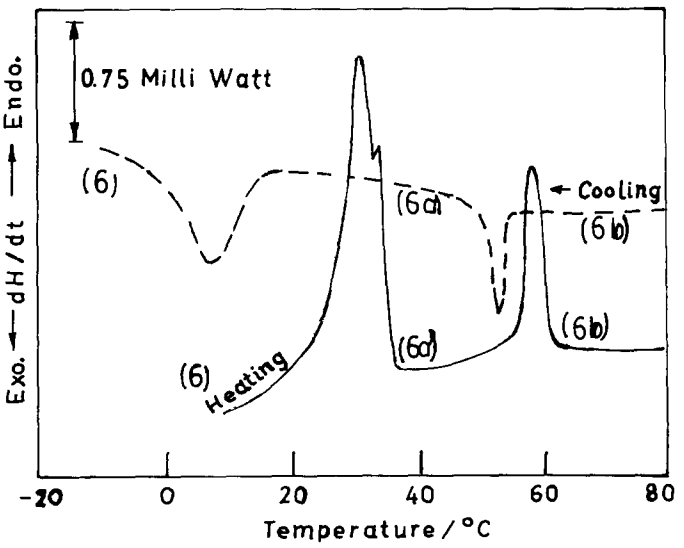

Fig. 2. DSC curves: $[NiL_3](NO_3)_2$ (**6**) (sample mass, 8.43 mg) (heating cycle, ——; cooling cycle, -----).

Table 4
Prominent lines (d/Å) in the X-ray powder diffraction patterns of the complexes

$[NiL_3]SO_4$ (7)[a]	$[NiL_3]SO_4$ (7a)
7.62 vs	7.75 vs
6.23 vs	5.86 vs
4.66 s	4.71 w
4.41 vw	4.45w
3.96 vw	3.57 s
3.83 vs	3.20 vw
3.60 vw	2.96 vw
3.54 vs	2.82 w
2.83 s	2.25 vw
2.79 w	2.02 vw
2.02 w	1.94 vw

[a] s, strong; w, weak, vs, very strong, vw, very weak.

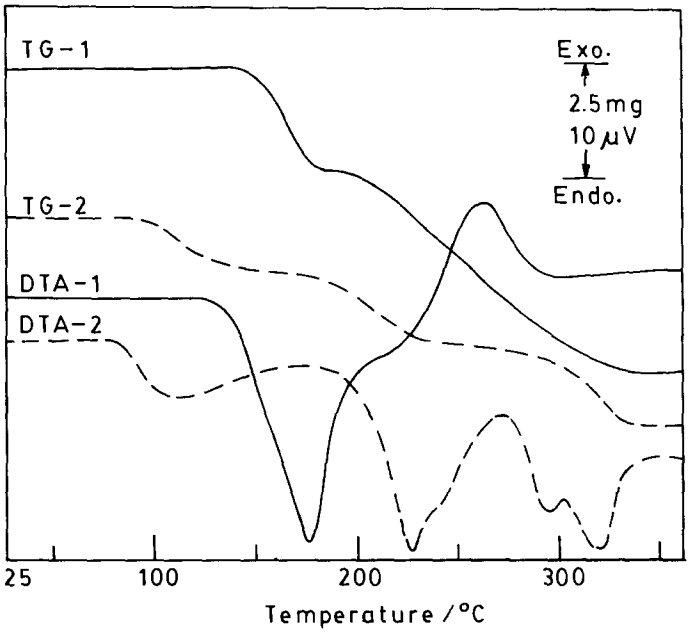

Fig. 3. TG–DTA curves: —, $[NiL_3]Cl_2$ (1) (sample mass, 12.01 mg); and ----; $[NiL_2Cl_2]$ (2) (sample mass, 10.60 mg).

in their TG curves indicating the formation of NiL_2Cl_2 and NiL_2SO_4, respectively, (Fig. 3 and 4). On the other hand, among the bis species only NiL_2Cl_2 (2) decomposes through the formation of intermediates, $NiL_{1.5}Cl_2$ and $NiLCl_2$ as evident from its TG curve (Fig. 3).

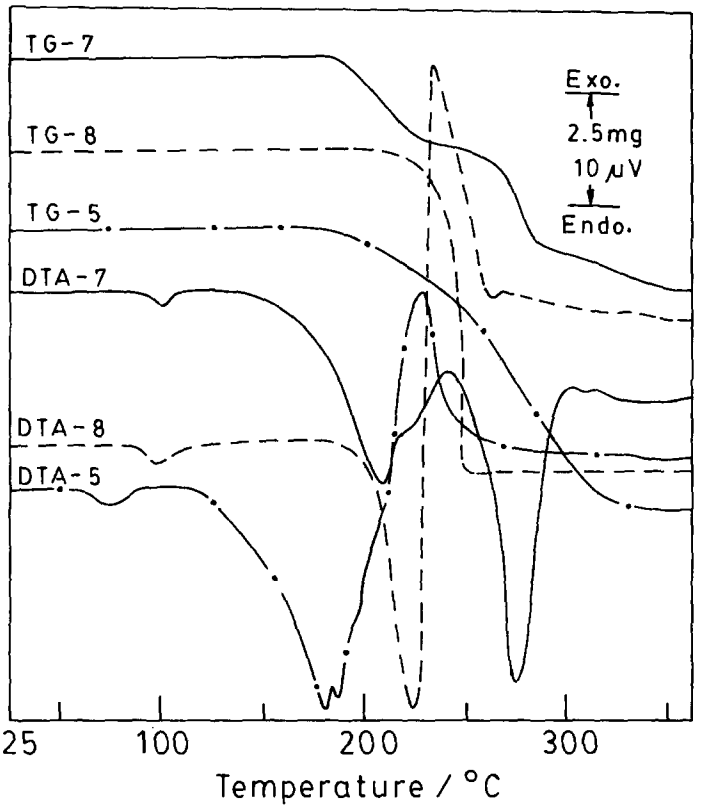

Fig. 4. TG–DTA curves: —, $[NiL_3]SO_4$ (7) (sample mass, 12.11 mg); ---, $[NiL_3]SeO_4$ (8) (sample mass, 12.25 mg); and – · –, $[NiL_3]I_2$ (5) (sample mass, 16.50 mg).

Table 5
Initial decomposition temperatures, T_i/(°C) of $[NiL_3]X_2$

	X				
L	Cl^{-1}	Br^{-1}	I^{-1}	$0.5SO_4^{2-}$	$0.5SeO_4^{2-}$
Ethane-1,2-diamine [4,5,19]	190	210	250	265	305
2-Aminoethanol	150	170	180	185	210

The thermal stability of the tris species varies with changing anions and the stability order is as follows: $Cl^- < Br^- < I^- < SO_4^{2-} < SeO_4^{2-}$ (Table 5). A similar trend is also observed for ethane-1,2-diamine. It is interesting to note that the complexes of 2-aminoethanol are found to be thermally less stable than those of ethane-1,2-diamine, as is evident from the T_i data (T_i = initial temperature of decomposition) (Table 5). The

intermediate species formed by the complexes of 2-aminoethanol are fewer are formed by ethane-1,2-diamine complexes of nickel(II). This can be attributed to the lower coordinating power of –OH group of 2-aminoethanol.

Acknowledgements

We are grateful to the Department of Geological Sciences, Jadavpur University and to the Polymer Science Unit, Indian Association for the Cultivation of Science, Jadavpur, Culcutta-700 032 for carrying out the X-ray powder diffraction study and the calorimetric study, respectively. We also thank Professor R. Ikeda, University of Tsukuba, Japan for high temperature IR spectra.

References

[1] W.W. Wendlandt and J.P. Smith, The Thermal Properties of Transition Metal Ammine Complexes, Elsevier, 1967, pp. 148–153.
[2] R. Tsuchiya, S. Joba, A. Uehara and E. Kyuno, Bull. Chem. Soc. Jpn., 46 (1973) 1454.
[3] Y. Ihara Y. Satake, M. Suzuki and A. Uehara, Bull. Chem. Soc. Jpn., 64 (1991) 3647 and references cited therein.
[4] G. De, P.K. Biswas and N. Ray Chaudhuri, Bull. Chem. Soc. Jpn., 56 (1983) 3145.
[5] D. Das, A. Ghosh and N. Ray Chaudhuri, Bull. Chem. Soc. Jpn., 67 (1994) 3254 and references cited therein.
[6] G. De, P.K. Biswas and N. Ray Chaudhuri, J. Chem. Soc. Dalton Trans., (1984) 2591.
[7] A.K Mukherjee, M. Mukherjee, A.J. Welch, A. Ghosh, G. De and N. Ray Chaudhuri, J. Chem. Soc. Dalton Trans., (1987) 997.
[8] S. Koner, A. Ghosh and N. Ray Chaudhuri, J. Chem. Soc. Dalton Trans., (1990) 1563.
[9] I. Ihara and R. Tsuchiya, Bull. Chem. Soc. Jpn., 57 (1984) 2829.
[10] D. Das, A. Ghosh, C. Pariya and N. Ray Chaudhuri, J. Chem. Research(S) (1994) 136.
[11] C. Pariya, A. Ghosh and N. Ray Chaudhuri, J. Chem. Research(S) (1994) 428.
[12] D.M.L. Goodgame and L.M. Venanzi, J. Chem. Soc. (1963) 616.
[13] M.S. Masoud, J. Inorg. Nucl. Chem., 39 (1977) 413.
[14] G.F. Svatos, C. Curran and J.V. Quagliano, J. Am. Chem. Soc., 77 (1955) 6159.
[15] M.B. Hursthouse, K.J. Izod, M.A. Mazid and P. Thornton, Polyhedron, 9 (1990) 535.
[16] G. De, P.K. Biswas and N. Ray Chaudhuri, J. Chem. Soc. Dalton Trans., (1984) 2591.
[17] A.K. Mukherjee, M. Mukherjee, S. Ray, A. Ghosh and N. Ray Chaudhuri, J. Chem. Soc. Dalton Trans., (1990) 2347.
[18] S. Koner, A. Ghosh and N. Ray Chaudhuri, Bull. Chem. Soc. Jpn., 63 (1990) 2387.
[19] S. Mitra, G. De and N. Ray Chaudhuri, Thermochim. Acta, 71 (1983) 107.